Published in final edited form as:
Biomaterials. 2012 November ; 33(31): . doi:10.1016/j.biomaterials.2012.07.010.

Effect of bone marrow-derived extracellular matrix on cardiac function after ischemic injury

Swathi Ravi[a], **Jeffrey M. Caves**[b,c,d], **Adam W. Martinez**[a], **Jiantao Xiao**[b], **Jing Wen**[b], **Carolyn A. Haller**[b,c,d], **Michael E. Davis**[a], and **Elliot L. Chaikof**[a,b,c,d,*]

[a] Department of Biomedical Engineering, Georgia Institute of Technology/Emory University, Atlanta, GA 30332, USA

[b] Department of Surgery, Emory University, Atlanta, GA 30322, USA

[c] Department of Surgery, Beth Israel Deaconess Medical Center, Harvard Medical School, Boston, MA 02215, USA

[d] Wyss Institute of Biologically Inspired Engineering, Harvard University, Boston, MA 02215, USA

Abstract

Ischemic heart disease is a leading cause of death, with few options to retain ventricular function following myocardial infarction. Hematopoietic-derived progenitor cells contribute to angiogenesis and tissue repair following ischemia reperfusion injury. Motivated by the role of bone marrow extracellular matrix (BM-ECM) in supporting the proliferation and regulation of these cell populations, we investigated BM-ECM injection in myocardial repair. In BM-ECM isolated from porcine sternum, we identified several factors important for myocardial healing, including vascular endothelial growth factor, basic fibroblast growth factor-2, and platelet-derived growth factor-BB. We further determined that BM-ECM serves as an adhesive substrate for endothelial cell proliferation. Bone marrow ECM was injected in a rat model of myocardial infarction, with and without a methylcellulose carrier gel. After one day, reduced infarct area was noted in rats receiving BM-ECM injection. After seven days we observed improved fractional shortening, decreased apoptosis, and significantly lower macrophage counts in the infarct border. Improvements in fractional shortening, sustained through 21 days, as well as decreased fibrotic area, enhanced angiogenesis, and greater c-kit-positive cell presence were associated with BM-ECM injection. Notably, the concentrations of BM-ECM growth factors were 10^3–10^8 fold lower than typically required to achieve a beneficial effect, as reported in pre-clinical studies that have administered single growth factors alone.

Keywords

Bone marrow; Growth factors; ECM (extracellular matrix); Heart; Thermally responsive material; Porcine tissue

1. Introduction

The development of an effective therapy to improve cardiac function following acute myocardial infarction (MI) has been elusive, even as ischemic heart disease is projected to

* Corresponding author.110 Francis St, Suite 9F, Boston, MA 02215, USA. Tel.: +1617 632 9581. echaikof@bidmc.harvard.edu (E.L. Chaikof)..

remain the leading global cause of death for decades to come [1]. The inability of myocardial tissue to regenerate results in negative left ventricular remodeling and dilation after a myocardial infarction, ultimately leading to heart failure. Cellular transplantation and regenerative medicine could enable minimally invasive alternatives to heart transplantation and left ventricular assist devices for treatment of heart failure. Injections of cells suspended in saline or in situ-gelling biomaterial carriers, as well as acellular biomaterial injections all represent feasible solutions with innate advantages and limitations.

Injectable materials recapitulating the appropriate mechanical cues in load-bearing tissues, and also releasing healing chemical or biologic factors, are of significant interest in regenerative medicine and cardiac tissue engineering. Beyond cell therapy, an expanding spectrum of synthetic polymer or biopolymer candidate injectables, sometimes augmented with growth factors, drugs, or cellular suspensions, have been reported for myocardial injection with the objective of curbing negative remodeling and loss of ventricular function [2]. Other general therapeutic goals in this field include diminished inflammation or scarring, improved angiogenesis and perfusion of the infarct area, stem cell recruitment, and myocardial tissue regeneration.

The extracellular matrix is a meshwork of fibrous proteins surrounded by glycosaminoglycans, growth factors, and sequestered cytokines. Extracellular matrices provide structural and signaling cues that organize and regulate cellular activity, leading to tissue repair and homeostasis, and thus can be utilized as natural biomaterials for regenerative medicine. For example, decellularized small intestinal submucosa (SIS) has been used extensively for wound healing and tissue regeneration [3]. Gels derived from decellularized SIS [4], myocardium [5], or pericardium [6] all demonstrate potential for tissue regeneration and functional improvement upon myocardial injection.

In this study, we examined bone marrow extracellular matrix (BM-ECM) for cardiac repair due to its unique role in supporting and regulating various stem cell populations in tissue maintenance and repair. The complex array of environmental cues associated with BM-ECM include fibronectin, collagen Types I, III, and IV, laminin, thrombospondin, hemonectin, and heparan sulfate proteoglycans and there is extensive evidence that different hematopoietic cell populations interact with distinct BM-ECM components [7]. Immature myeloid and erythroid cells have been shown to bind both to fibronectin [8] and collagen Type I [9], while CD34 progenitors bind to fibronectin in an activation-dependent manner [10]. Moreover, considerable evidence supports the notion that a unique ECM composition is critical in the development, regulation, and differentiation of cells derived from diverse hematopoietic lineages [11]. For example, Long et al. [7] have demonstrated that thrombospondin and c-kit ligand function as a co-immobilized signaling complex regulating hematopoietic stem cell development and Bruno et al. [12] have shown that the binding of hematopoietic progenitor cells to GM-CSF and IL-3 is dependant upon their association with heparan sulfate proteoglycans.

In addition to ECM proteins, others mediators of homing found within the bone marrow include SDF-1, sphingosine-1-phosphate, VEGF, complement, and wingless-related (WNT) proteins. Indeed, many of these same compounds appear to recruit progenitor cells to acutely ischemic tissue, the severely injured vessel wall, and tumor neovasculature when released locally at these sites. While many of the factors appear to be responsible for promoting neovascularization, as well as the repair of intimal defects through direct recruitment of endothelial progenitor cells (EPCs), recent investigations have demonstrated that newly arrived EPCs also release proangiogenic factors in a paracrine manner that enhances the efficiency of these processes.

This work was based upon the postulate that BM-ECM contains both matrix and non-matrix factors that drive homing and survival of hematopoietic-derived endothelial progenitor cells as well as endothelial cell migration and proliferation. The synergistic effects of cardiomyocyte pro-survival signals, anti-inflammatory cues, recruitment and homing cues for stem cell infiltration, and angiogenic mediators within the bone marrow ECM, when delivered in a localized manner over a sustained period of time, may serve as an effective therapy for myocardial infarction.

2. Materials and methods

2.1. Isolation and purification of porcine bone marrow-derived extracellular matrix

Bone marrow was acquired from porcine sternums harvested from young adult swine that were 6–7 months of age and in ranging in weight between 240 and 290 lbs. The marrow was cut into small segments in order to be ground in a bone mill. The samples were stored at –80 °C prior to processing. The milled material was purified by adding DNase working solution with 5X antibiotic-antimycotic to approximately 5 g of marrow and incubating at 35 rpm for 1 h at 37 °C. The DNase solution was decanted and PBS containing 1X protease arrest, 5 mM EDTA, and 1X antibiotic-antimycotic was added to the remaining material. The extracellular matrix was then sheared off the bone marrow using a mini-vortexer, and the ECM-containing supernatant was transferred to a fresh tube. To recover any additional ECM, the PBS solution was once again added to the marrow for a secondary vortex cycle. Bone fragments were allowed to settle for 5 min before transferring the ECM-containing supernatant to a new tube. To isolate the ECM, the material was centrifuged at 10,000 rcf for 10 min at 4 °C. After decanting the liquid from the tube, the ECM pellet was resuspended in DNase working solution with 1X antibiotic for a secondary DNase digestion, with an incubation time of 2 h performed at 50 rpm and 37 °C, followed by another spin cycle. The supernatant was carefully discarded and the pellet was resuspended in PBS.

The ECM slurry was further purified from bone fragments using a sucrose gradient. Solutions of 50% sucrose were dispensed into labeled spin tubes followed by pipetting ECM over the sucrose layer so as to not disrupt the interface between the two solutions. Centrifugation was performed at 200 rcf for 10 min at 4 °C. The brown-white ECM band was then collected and placed in a sterile tube. Distilled water containing antibiotic was mixed with the slurry and contaminants were removed by centrifugation at 4200 rcf for 20 min followed by discarding the supernatant. This spin cycle was repeated until a clear pellet was observed. A final PBS wash was performed on the ECM pellet prior to centrifugation. The material was diluted in PBS containing 100 mg/L calcium chloride and magnesium chloride using the weight of the pellet for volume in preparation for further studies.

2.2. Characterization of bone-marrow ECM (BM-ECM)

BM-ECM was analyzed by SDS-PAGE by running 3 μg of ECM on a 3–8% Tris-acetate gel (Biorad Laboratories) in XT Tricine running buffer along with a molecular weight marker (Himark unstained protein standard, Invitrogen) followed by silver staining. Growth factor content was quantified using Quantikine Fibroblast Growth Factor (FGF-basic) and Human Platelet-derived Growth Factor-BB (PDGF-BB) immunoassays (R&D Systems). sGAG content was determined using the Blyscan sulfated glycosaminoglycan assay (Biocolor, Ltd) and DNA content defined using the Picogreen dsDNA assay (Invitrogen).

2.3. Preparation of methylcellulose and BM-ECM for local delivery

Methylcellulose (MC) solutions (8 wt%) were formed by a dispersion technique. Briefly, half of the required volume of PBS containing magnesium and calcium was heated above 60 °C. Methylcellulose powder was added to the heated solvent and vortexed for 1 min until all

polymer particles were thoroughly wetted. The remaining PBS volume, chilled on ice, was then added to the methylcellulose paste. After vortexing for another minute, the mixture was placed on ice for 1 h, after which the polymer solution became clear and increased in viscosity. The sample was then lightly agitated for another 2 h at 4 °C. The uniform solution was sterile-filtered through a 0.22 μm syringe filter (Millipore). For formulations containing bone marrow-ECM (ECM-MC), varying ECM concentrations were added to filtered methylcellulose solutions. The entire mixture was allowed to equilibrate by stirring gently overnight at 4 °C. ECM-only formulations were diluted in 1X PBS.

2.4. Rheological analysis

Rheological analysis of 8wt% MC and 8wt% MC containing 300 μg/mL ECM was performed to determine gelation temperatures and viscoelastic behavior. Data was acquired on an Advanced Rheological Expansion System III rheometer (ARES III, TA Instrument, NJ) in parallel plate geometry with a plate diameter of 25 mm. Sample solutions were prepared as detailed above. The gap between the parallel plates was adjusted between 0.2 and 0.35 mm and dynamic mechanical experiments were performed in shear deformation mode. Samples were heated from 4 °C to 40 °C at a rate of 1 °C per minute, frequency of 1 Hz, and fixed strain amplitude of 2%.

2.5. In vitro cell studies

ECM slurry at varying concentrations was allowed to passively adsorb overnight at 4 °C onto non-tissue culture-treated polystyrene 48-well plates followed by rinsing the wells with PBS. Fibronectin (50 μg/mL) was adsorbed onto well surfaces in a similar manner. Blocking non-specific interactions was achieved by treating wells with 1% heat inactivated bovine serum albumin (BSA) for a 1 h period followed by PBS rinsing. Wells treated with BSA only were used as non-cell adhesive reference substrates. MC and ECM-MC gels were produced by casting 200 μL of each solution into the wells of a 48-well non-tissue culture-treated polystyrene plate, which were then incubated at 37 °C for 4 h prior to cell seeding.

Human umbilical vein endothelial cells (HUVECs) were purchased from Clonetics and maintained in endothelial growth medium-2 (EGM-2, 2% serum, Clonetics) in a humidified, 5% CO_2 environment at 37 °C. HUVECs were used between passages 3 and 10 for all experiments. Cells were harvested with Cell Dissociation Solution (EDTA, glycerol, sodium citrate, PBS, Sigma) in order to maintain integrin functionality on the cell surface. After centrifugation at 220 g for 5 min, suspensions were prepared at a density of 500,000 cells/mL in basal medium containing no serum. A total of 100 μL of cell suspension was plated into each well and after a 2 h incubation period, wells were washed in PBS to remove non-adherent cells. Cell attachment was evaluated using the CyQuant Cell Proliferation Assay Kit (Molecular Probes) and normalized to levels on fibronectin-coated polystyrene surfaces.

HUVEC proliferation was followed over a 96-h period. Cells were seeded in non-serum containing medium onto various substrates at a density of 2000 cells per well for 6 h to ensure adhesion. Unbound cells were removed with media washes and substrate-bound cells were maintained in culture for another 4 d in serum-containing media. Fresh media was replaced in each well every 48 h. The CyQuant Cell Proliferation Assay Kit was utilized to assess cell number at 6, 48, and 96 h.

Haptotactic migration was evaluated using a Boyden chamber assay (Transwell filters, 80 μm pore size). HUVECs were initially serum starved for 16 h. Serum-free media with varying concentrations of bone marrow ECM was placed in the lower well, while the upper chamber of each well insert was seeded with 80,000 cells. The use of serum-free media containing 10% FBS served as a positive control. Cells were allowed to migrate across

inserts for 6 h at 37 °C. Cells were fixed in 10% formal-dehyde and stained in hematoxylin, after which the upper membrane surface was swabbed with a wet cotton swab and rinsed in distilled, deionized water. The average number of migrated cells in six randomly chosen 40× magnification fields of view per insert was taken to quantify the extent of migration. In addition, the experiment was run in triplicate.

2.6. Rat coronary artery ischemia reperfusion model

Adult male Sprague–Dawley rats weighing 250 g were purchased from Charles River Laboratories. Briefly, animals were anesthetized (1–3% isoflurane) and, following tracheal intubation, hearts were exposed by separation of the ribs. Myocardial infarction was induced by transient ligation of the left descending coronary artery for 30 min followed by reperfusion. Immediately after exposure of the heart (sham studies) or ischemia reperfusion, one of three formulations was injected into the infarct zone consisting of the free wall of the left ventricle through a 30-gauge needle while the heart was beating. A total of 50 μL of 8wt % MC, 8wt% MC containing 300 μg/mL ECM, or a solution of 300 μg/mL of ECM alone were injected. Chests were then closed and animals allowed to recover on a heating pad. All studies were conducted using a randomized and blinded protocol with rats enrolled in sham surgery or undergoing ischemia reperfusion without treatment, serving as negative and positive control groups, respectively.

Cardiac function was assessed using echocardiography 7 and 21 d after infarction. Specifically, fractional shortening was derived from the end-diastolic dimension and end-systolic dimension. Myocardial infarct size was evaluated using 2,3,5-triphenyltetrazolium chloride (TTC) staining and Evans Blue dye in which the percent area of infarctionwas calculated as the infarcted area (TTC stained) divided by the ischemic area at risk (Evans Blue stained). For immunohistological evaluation, hearts were harvested and fixed in 4% paraformaldehyde prior to being embedded in paraffin and sectioned into 5 μm thick samples. Collagen deposition was determined by Picrosirius Red (Sigma) staining. Macrophage infiltration was identified using CD68 monoclonal antibody (Abcam). Apoptosis was detected with the CardioTACS *in situ* apoptosis detection kit (Trevigen). Digital images and area measurements were obtained in a blinded manner. Angiogenesis was detected by Von Willebrand Factor antibody staining (Abcam, ab6994). C-kit-positive cells were identified with H-300 ckit antibody (Santa Cruz Biotechnology).

2.7. Statistics

Comparison between groups was analyzed via ANOVA and a paired, two-tailed student's *t*-test, with $p < 0.05$ considered to be significant. Results are presented as mean standard deviation. For in vitro studies, data represent characteristic results from a particular experimental run, with each group run at least in quadruplicate and a minimum of three independent runs conducted. For in vivo studies, four rats were enrolled in each treatment group.

3. Results

3.1. In vitro characterization of bone marrow-derived extracellular matrix

Gel electrophoresis revealed the presence of a range of proteins and ECM fragments, and further analysis was performed on selected components of interest (Fig. 1A, B). Extracellular matrix-bound growth factors work in concert to regulate cell migration, proliferation, and differentiation through the repair process. Therefore, to identify those growth factors that could be responsible for BM-ECM induced tissue regeneration, porcine ELISAs were performed for FGF-2, PDGF-BB, and TGF-β1, as listed in Fig. 1B.

Furthermore, using a Blyscan assay, the glycosaminoglycan content of the matrix was determined. The dsDNA content in the BM-ECM was 198 ± 110 μg per mg of ECM.

3.2. Rheological analysis of methylcellulose formulations

We investigated intramyocardial injections of both methylcellulose (MC) and ECM-methylcellulose (ECM-MC) compositions, which undergo a sol–gel transition upon heating. Storage modulus, loss modulus, dynamic viscosity, and tan δ were obtained from rheological measurements and were plotted as a function of temperature (Fig. 2A, B). At the gelation temperature, the loss and storage modulus increase sharply, while tan δ decreases, consistent with the formation of a viscoelastic gel. Gelation temperatures derived from the point of maximum slope of the dynamic viscosity curve for MC and ECM-MC were 30.9 ± 1.4 °C and 26.5 ± 0.9 °C, respectively ($p < 0.05$), which ensured *in situ* gelation of these solutions upon microinjection at 37 °C.

3.3. Cell adhesion and proliferation in vitro

Human endothelial cell adhesion was initially characterized in a standard 2 h adhesion assay on non-tissue culture-treated wells pretreated by overnight incubation at 4 °C to ECM (30–3000 μg/mL) or fibronectin (50 μg/mL). Surfaces incubated with ECM concentrations equal to or greater than 30 μg/mL were able to support robust cell attachment (Fig. 3A). Likewise, a 9-fold increase in cell number was observed over a 96-h period when cells were incubated in wells pretreated with ECM concentrations equal to or exceeding 300 μg/mL (Fig. 3B). Consistent with these results, a significant haptotactic response was observed on surfaces exposed to similar ECM concentrations (Fig. 3E).

Cell adhesion and proliferation was subsequently assessed on substrates coated with MC with or without incorporated ECM. MC formulations (8wt%) that contained 30 μg/mL of ECM were insufficient to support a significant adhesive response (Fig. 3C). However, when ECM concentrations were 300 μg/mL or higher, gels displayed adhesive responses were statistically equivalent to those observed on fibronectin-coated surfaces. Similar formulations supported an 11-fold increase in cell number over a 96-h incubation period.

3.4. Post-MI injection of ECM-MC

The extent of the myocardial infarction was evaluated at 24 h after injury using TTC staining and Evans Blue dye (Fig. 4B). A 53% reduction in the ischemic area was noted among rats treated with the ECM-MC formulation as compared to other treatment groups. A reduction in infarct area was not observed when treated with ECM alone. Cardiac function was assessed using echocardiography at 7 and 21 d after induction of myocardial infarction (Fig. 4A). At 7 d, both ECM and ECM-MC treated rats showed improvement in fractional shortening when compared to those rats subjected to ischemia reperfusion in the absence of treatment. However, at 21 d, only those treated with an ECM-MC formulation demonstrated significant improvement in fractional shortening. Macrophage infiltration in the border zone and apoptosis at 7 d were significantly reduced only in the ECM-MC treatment group (Fig. 5).

Late functional improvement at 21 d may be related to reduced fibrosis or enhanced myocardial repair consistent with the recruitment of cardiac progenitor cells or an angiogenic response. Fibrosis, defined histologically by Picrosirius Red staining for collagen deposition, was significantly reduced in those groups treated with ECM or ECM-MC (Fig. 6). The density of c-kit-positive cells and blood vessels in the border zone of the infarct area were both substantially greater among those animals treated with ECM-MC. The MC vehicle and ECM alone were unable to promote an angiogenic response (Fig. 7).

4. Discussion

Emphasis on the development of injectable gels for myocardial repair has increased following observations that fibrin glue injections decreased infarct scar size and prevented declines in fractional shortening [13,14]. Although cardiomyocyte or progenitor cell transplant would seem the most direct path to restored function, low levels of cellular engraftment currently detract from this strategy. A wide range of biomaterial gels designed for intramyocardial injection have been reported and reviewed [2,15]. These materials may act as mechanical bulking agents, decreasing the average stress on the ventricular wall by increasing wall thickness. Alternatively, various biopolymers may induce cellular ingrowth and angiogenesis through innate bioactive sites, or may be engineered to release growth factors or drugs. Compared to cell therapy, this class of injectables could prove a more translatable and scalable solution for the large patient population suffering from negative LV remodeling [16].

Reports suggest that acellular, ECM-derived implants have the capacity to guide macrophage immunomodulatory responses [17], recruit progenitor cells [18], and remodel into organized, functional tissues [19–21]. These observations are attributed to bioactive molecules or peptide fragments released upon scaffold degradation, which promote migration, proliferation, and differentiation of progenitor cells from the circulation or adjacent tissues. Our understanding of this process remains incomplete, and only a few studies have examined the case of ECM-derived injectables for myocardial repair. Suspensions of acellular small intestinal submucosa (SIS) have been shown to improve function, increase levels of stem cell factor, VEGF, c-kit-positive cells, myofibroblasts, and macrophages [22]. When other SIS gels were injected in ischemic mouse myocardium, a variant with greater FGF-2 content was correlated to an enhanced biologic and therapeutic effect [4]. Matrices from myocardium and pericardium have also been reported to promote EC and SMC infiltration, and neovascularization, following injection into non-infarcted rat hearts [5,6]. These matrices contained a range of anticipated ECM components, including several collagen types, sGAG, and elastin.

In BM-ECM, we have identified detectable levels of a collection of growth factors prominent in myocardial repair. Several have demonstrated efficacy in myocardial injection studies. Vascular endothelial growth factor has been investigated extensively in myocardial repair, although side effects underscore the significance of controlled and localized delivery [23]. Fibroblast growth factor-2 is associated with cell proliferation, angiogenesis, cardiomyocyte differentiation, and scar contraction following MI [24,25]. Studies combining FGF-2 with gelatin [26], chitosan [27,28], or a copolymer hydrogel [29] report reduced infarct size, increased angiogenesis, and functional gains. Various isoforms of PDGF are associated with angiogenesis as well as cardiomyocyte survival and differentiation [30–33]. Sustained release of insulin-like growth factor (IGF-2), when combined with cardiomyocyte injection, increased myocyte size and improved systolic function [34]. Any of these factors, their combination, or the presence of other non-defined constituents may be responsible for the effect of BM-ECM. Notably, the concentration of BM-ECM growth factors were 10^3–10^8 fold lower than typically required to achieve a beneficial effect, as reported in pre-clinical studies that have administered single growth factors alone. For example, FGF has been administered in rat MI models at doses of 2–100 μg [26,27,29,35], but the dose in the present study was 1.1 pg. Similarly, PDGF has been administered in amounts ranging from 4 ng to 3 μg [30–33], compared 1.2 pg in this study. In swine [36] and rat [33] models, VEGF was effective in doses of 20 μg and 3 μg, respectively, levels considerably greater than the estimated level of 0.01 pg in BM-ECM. Therefore, the efficacy of BM-ECM may not be exclusive to any one of these factors, but to their combined effect, with additional contributions from unidentified components. Indeed,

all of the growth factors that were quantified in the BM-ECM are known to interact synergistically with other factors. For example, VEGF and FGF-2 have a combined angiogenic effect greater than the sum of their individual contributions [37]. TGF-β1 upregulates transcription of FGF-2 and VEGF by smooth muscle cells, but also accentuates the effect of these factors in vitro in the absence of smooth muscle cells [38–40]. In addition, combinations of PDGF-BB and IGF-1 have a coordinated effect, increasing collagen fiber deposition and alignment in wound healing [41,42]. In principle, the low growth factor concentrations observed in BM-ECM may limit undesirable effects associated with growth factor administration.

In this study, the mechanical or bulking effect and the bioactivity are attributed to separate components, providing insight into the relative significance of these two phenomena. We employed MC as a versatile biopolymer that undergoes *in situ* gelation due to hydrophobic interactions attributed to the methoxy substitution that drive a sol–gel phase transition that is tunable through adjustment of MC and salt concentrations [43]. Prior in vivo studies have reported the application of MC as a biodegradable carrier agent for sustained growth factor delivery without significant inflammatory response in central or peripheral nervous system sites [43,44].

Following myocardial infarction, ventricular wall thinning is associated with increased wall stress and negative left ventricular remodeling. Computational modeling has suggested that gels injected as bulking agents can alter the stress distribution in the ventricular wall and alleviate negative remodeling [45]. Although many injectables have shown benefit, in almost all cases these interventions have a biological effect, which cannot be clearly decoupled from mechanical bulking [2,46]. Indeed, injection of an inert polyethylene glycol gel showed no prolonged benefit [47]. We also observed no benefit from MC alone, either because the effect of mechanical bulking was small, ordue to degradation of the MC. Notably, this study did not establish a time course for degradation of the MC. Although such studies will be required in the future, quantification of MC degradation in vivo is challenging due to temperature driven reversal of gelation when tissue samples are harvested and processed [43].

Macrophage infiltration immediately following myocardial injury results in cell debris clearance and secretion of VEGF and TGF-β, followed by improved neovascularization, collagen deposition, and wound healing [48,49]. However, extended macrophage persistence is a hallmark of chronic inflammation, and likely to be detrimental to later stages of ventricular remodeling [49]. Indeed, pharmacologic reduction of macrophage infiltration has been correlated to reduced fibrosis and improved fractional shortening [50]. Here, we observed lower macrophage levels after 7 d following EMC-MC injection. Because this treatment also led to improved functional outcomes, greater angiogenesis, and reduced apoptosis, we speculate that the lower macrophage level indicates a diminished pro-inflammatory macrophage population [51].

Our observation that c-kit-positive cell accumulation is correlated with more extensive angiogenesis is consistent with the reported role of these cells in myocardial repair. Bone marrow cells expressing c-kit, including hematopoietic stem cells and endothelial progenitor cells, have been associated with initiation of angio-genesis and tissue repair [52]. Injected c-kit-positive bone marrow cells have also been shown to transdifferentiate into cardiomyocytes, contributing mechanically and electrically to heart function [53]. Although c-kit is also expressed on resident cardiac progenitor cells, in the context of MI repair the majority of c-kit-positive cells are reported to be bone marrow-derived [52], underscoring the significance of a potential supportive role for BM-ECM in intramyocardial injection.

5. Conclusion

Our salient findings were that ECM-MC therapy improved cardiac function and reduced infarct and fibrotic areas. We also noted the presence of several bioactive molecules in BM-ECM, although concentrations were 10^3–10^8 fold lower than typically required to achieve a beneficial effect. Compared to BM-ECM alone, combining the matrix with a methylcellulose carrier gel resulted in smaller infarct areas and prolonged improvements in fractional shortening. The composite injection also increased angiogenesis and c-kit-positive cell accumulation, and reduced apoptosis and macrophage levels in the infarct border zone.

Acknowledgments

This project was funded by a grant from the Boston Scientific Corporation.

References

1. Mathers CD, Loncar D. Projections of global mortality and burden of disease from 2002 to 2030. PLoS Med. 2006; 3:e442. [PubMed: 17132052]
2. Tous E, Purcell B, Ifkovits JL, Burdick JA. Injectable acellular hydrogels for cardiac repair. J Cardiovasc Transl Res. 2011; 4:528–42. [PubMed: 21710332]
3. Badylak SF. The extracellular matrix as a biologic scaffold material. Biomaterials. 2007; 28:3587–93. [PubMed: 17524477]
4. Okada M, Payne TR, Oshima H, Momoi N, Tobita K, Huard J. Differential efficacy of gels derived from small intestinal submucosa as an injectable biomaterial for myocardial infarct repair. Biomaterials. 2010; 31:7678–83. [PubMed: 20674011]
5. Singelyn JM, DeQuach JA, Seif-Naraghi SB, Littlefield RB, Schup-Magoffin PJ, Christman KL. Naturally derived myocardial matrix as an injectable scaffold for cardiac tissue engineering. Biomaterials. 2009; 30:5409–16. [PubMed: 19608268]
6. Seif-Naraghi SB, Salvatore MA, Schup-Magoffin PJ, Hu DP, Christman KL. Design and characterization of an injectable pericardial matrix gel: a potentially autologous scaffold for cardiac tissue engineering. Tissue Eng Part A. 2010; 16:2017–27. [PubMed: 20100033]
7. Long MW, Briddell R, Walter AW, Bruno E, Hoffman R. Human hematopoietic stem cell adherence to cytokines and matrix molecules. J Clin Invest. 1992; 90:251–5. [PubMed: 1378855]
8. Giancotti FG, Comoglio PM, Tarone G. Fibronectin-plasma membrane interaction in the adhesion of hemopoietic cells. J Cell Biol. 1986; 103:429–37. [PubMed: 2942550]
9. Koenigsmann M, Griffin JD, DiCarlo J, Cannistra SA. Myeloid and erythroid progenitor cells from normal bone marrow adhere to collagen type I. Blood. 1992; 79:657–65. [PubMed: 1370640]
10. Kerst JM, Sanders JB, Slaper-Cortenbach IC, Doorakkers MC, Hooibrink B, van Oers RH, et al. Alpha 4 beta 1 and alpha 5 beta 1 are differentially expressed during myelopoiesis and mediate the adherence of human CD34+ cells to fibronectin in an activation-dependent way. Blood. 1993; 81:344–51. [PubMed: 7678511]
11. Quesenberry P, Song ZX, McGrath E, McNiece I, Shadduck R, Waheed A, et al. Multilineage synergistic activity produced by a murine adherent marrow cell line. Blood. 1987; 69:827–35. [PubMed: 3493043]
12. Bruno E, Luikart SD, Long MW, Hoffman R. Marrow-derived heparan sulfate proteoglycan mediates the adhesion of hematopoietic progenitor cells to cytokines. Exp Hematol. 1995; 23:1212–7. [PubMed: 7556532]
13. Christman KL, Fok HH, Sievers RE, Fang Q, Lee RJ. Fibrin glue alone and skeletal myoblasts in a fibrin scaffold preserve cardiac function after myocardial infarction. Tissue Eng. 2004; 10:403–9. [PubMed: 15165457]
14. Christman KL, Vardanian AJ, Fang Q, Sievers RE, Fok HH, Lee RJ. Injectable fibrin scaffold improves cell transplant survival, reduces infarct expansion, and induces neovasculature formation in ischemic myocardium. J Am Coll Cardiol. 2004; 44:654–60. [PubMed: 15358036]

15. Singelyn JM, Christman KL. Injectable materials for the treatment of myocardial infarction and heart failure: the promise of decellularized matrices. J Cardiovasc Transl Res. 2010; 3:478–86. [PubMed: 20632221]

16. McAllister TN, Dusserre N, Maruszewski M, L'Heureux N. Cell-based therapeutics from an economic perspective: primed for a commercial success or a research sinkhole? Regen Med. 2008; 3:925–37. [PubMed: 18947313]

17. Badylak SF, Valentin JE, Ravindra AK, McCabe GP, Stewart-Akers AM. Macrophage phenotype as a determinant of biologic scaffold remodeling. Tissue Eng Part A. 2008; 14:1835–42. [PubMed: 18950271]

18. Beattie AJ, Gilbert TW, Guyot JP, Yates AJ, Badylak SF. Chemoattraction of progenitor cells by remodeling extracellular matrix scaffolds. Tissue Eng Part A. 2009; 15:1119–25. [PubMed: 18837648]

19. Kropp BP, Rippy MK, Badylak SF, Adams MC, Keating MA, Rink RC, et al. Regenerative urinary bladder augmentation using small intestinal submucosa: urodynamic and histopathologic assessment in long-term canine bladder augmentations. J Urol. 1996; 155:2098–104. [PubMed: 8618344]

20. Kochupura PV, Azeloglu EU, Kelly DJ, Doronin SV, Badylak SF, Krukenkamp IB, et al. Tissue-engineered myocardial patch derived from extracellular matrix provides regional mechanical function. Circulation. 2005; 112:I144–9. [PubMed: 16159807]

21. Valentin JE, Turner NJ, Gilbert TW, Badylak SF. Functional skeletal muscle formation with a biologic scaffold. Biomaterials. 2010; 31:7475–84. [PubMed: 20638716]

22. Zhao ZQ, Puskas JD, Xu D, Wang NP, Mosunjac M, Guyton RA, et al. Improvement in cardiac function with small intestine extracellular matrix is associated with recruitment of C-kit cells, myofibroblasts, and macrophages after myocardial infarction. J Am Coll Cardiol. 2010; 55:1250–61. [PubMed: 20298933]

23. Lee RJ, Springer ML, Blanco-Bose WE, Shaw R, Ursell PC, Blau HM. VEGF gene delivery to myocardium: deleterious effects of unregulated expression. Circulation. 2000; 102:898–901. [PubMed: 10952959]

24. Rosenblatt-Velin N, Lepore MG, Cartoni C, Beermann F, Pedrazzini T. FGF-2 controls the differentiation of resident cardiac precursors into functional cardiomyocytes. J Clin Invest. 2005; 115:1724–33. [PubMed: 15951838]

25. Virag JA, Rolle ML, Reece J, Hardouin S, Feigl EO, Murry CE. Fibroblast growth factor-2 regulates myocardial infarct repair: effects on cell proliferation, scar contraction, and ventricular function. Am J Pathol. 2007; 171:1431–40. [PubMed: 17872976]

26. Iwakura A, Fujita M, Kataoka K, Tambara K, Sakakibara Y, Komeda M, et al. Intramyocardial sustained delivery of basic fibroblast growth factor improves angiogenesis and ventricular function in a rat infarct model. Heart Vessels. 2003; 18:93–9. [PubMed: 12756606]

27. Wang H, Zhang X, Li Y, Ma Y, Zhang Y, Liu Z, et al. Improved myocardial performance in infarcted rat heart by co-injection of basic fibroblast growth factor with temperature-responsive chitosan hydrogel. J Heart Lung Transplant. 2010; 29:881–7. [PubMed: 20466563]

28. Fujita M, Ishihara M, Morimoto Y, Simizu M, Saito Y, Yura H, et al. Efficacy of photocrosslinkable chitosan hydrogel containing fibroblast growth factor-2 in a rabbit model of chronic myocardial infarction. J Surg Res. 2005; 126:27–33. [PubMed: 15916971]

29. Garbern JC, Minami E, Stayton PS, Murry CE. Delivery of basic fibroblast growth factor with a pH-responsive, injectable hydrogel to improve angio-genesis in infarcted myocardium. Biomaterials. 2011; 32:2407–16. [PubMed: 21186056]

30. Hsieh PC, Davis ME, Gannon J, MacGillivray C, Lee RT. Controlled delivery of PDGF-BB for myocardial protection using injectable self-assembling peptide nanofibers. J Clin Invest. 2006; 116:237–48. [PubMed: 16357943]

31. Edelberg JM, Lee SH, Kaur M, Tang L, Feirt NM, McCabe S, et al. Platelet-derived growth factor-AB limits the extent of myocardial infarction in a rat model: feasibility of restoring impaired angiogenic capacity in the aging heart. Circulation. 2002; 105:608–13. [PubMed: 11827927]

32. Xaymardan M, Tang L, Zagreda L, Pallante B, Zheng J, Chazen JL, et al. Platelet-derived growth factor-AB promotes the generation of adult bone marrow-derived cardiac myocytes. Circ Res. 2004; 94:E39–45. [PubMed: 14963008]
33. Hao X, Silva EA, Mansson-Broberg A, Grinnemo KH, Siddiqui AJ, Dellgren G, et al. Angiogenic effects of sequential release of VEGF-A165 and PDGF-BB with alginate hydrogels after myocardial infarction. Cardiovasc Res. 2007; 75:178–85. [PubMed: 17481597]
34. Davis ME, Hsieh PC, Takahashi T, Song Q, Zhang S, Kamm RD, et al. Local myocardial insulin-like growth factor 1 (IGF-1) delivery with biotinylated peptide nanofibers improves cell therapy for myocardial infarction. Proc Natl Acad Sci U S A. 2006; 103:8155–60. [PubMed: 16698918]
35. Shao ZQ, Takaji K, Katayama Y, Kunitomo R, Sakaguchi H, Lai ZF, et al. Effects of intramyocardial administration of slow-release basic fibroblast growth factor on angiogenesis and ventricular remodeling in a rat infarct model. Circ J. 2006; 70:471–7. [PubMed: 16565567]
36. Lopez JJ, Laham RJ, Stamler A, Pearlman JD, Bunting S, Kaplan A, et al. VEGF administration in chronic myocardial ischemia in pigs. Cardiovasc Res. 1998; 40:272–81. [PubMed: 9893720]
37. Asahara T, Bauters C, Zheng LP, Takeshita S, Bunting S, Ferrara N, et al. Synergistic effect of vascular endothelial growth factor and basic fibroblast growth factor on angiogenesis in vivo. Circulation. 1995; 92:II365–71. [PubMed: 7586439]
38. Pepper MS, Vassalli JD, Orci L, Montesano R. Biphasic effect of transforming growth factor-beta 1 on in vitro angiogenesis. Exp Cell Res. 1993; 204:356–63. [PubMed: 7679998]
39. Gajdusek CM, Luo Z, Mayberg MR. Basic fibroblast growth factor and transforming growth factor beta-1: synergistic mediators of angiogenesis in vitro. J Cell Physiol. 1993; 157:133–44. [PubMed: 7691833]
40. Brogi E, Wu T, Namiki A, Isner JM. Indirect angiogenic cytokines upregulate VEGF and bFGF gene expression in vascular smooth muscle cells, whereas hypoxia upregulates VEGF expression only. Circulation. 1994; 90:649–52. [PubMed: 8044933]
41. Lynch SE, Nixon JC, Colvin RB, Antoniades HN. Role of platelet-derived growth factor in wound healing: synergistic effects with other growth factors. Proc Natl Acad Sci U S A. 1987; 84:7696–700. [PubMed: 3499612]
42. Lynch SE, Colvin RB, Antoniades HN. Growth factors in wound healing. Single and synergistic effects on partial thickness porcine skin wounds. J Clin Invest. 1989; 84:640–6. [PubMed: 2788174]
43. Tate MC, Shear DA, Hoffman SW, Stein DG, LaPlaca MC. Biocompatibility of methylcellulose-based constructs designed for intracerebral gelation following experimental traumatic brain injury. Biomaterials. 2001; 22:1113–23. [PubMed: 11352091]
44. Wells MR, Kraus K, Batter DK, Blunt DG, Weremowitz J, Lynch SE, et al. Gel matrix vehicles for growth factor application in nerve gap injuries repaired with tubes: a comparison of biomatrix, collagen, and methylcellulose. Exp Neurol. 1997; 146:395–402. [PubMed: 9270050]
45. Wall ST, Walker JC, Healy KE, Ratcliffe MB, Guccione JM. Theoretical impact of the injection of material into the myocardium: a finite element model simulation. Circulation. 2006; 114:2627–35. [PubMed: 17130342]
46. Rane AA, Christman KL. Biomaterials for the treatment of myocardial infarction: a 5-year update. J Am Coll Cardiol. 2011; 58:2615–29. [PubMed: 22152947]
47. Rane AA, Chuang JS, Shah A, Hu DP, Dalton ND, Gu Y, et al. Increased infarct wall thickness by a bio-inert material is insufficient to prevent negative left ventricular remodeling after myocardial infarction. PLoS One. 2011; 6:e21571. [PubMed: 21731777]
48. van Amerongen MJ, Harmsen MC, van Rooijen N, Petersen AH, van Luyn MJ. Macrophage depletion impairs wound healing and increases left ventricular remodeling after myocardial injury in mice. Am J Pathol. 2007; 170:818–29. [PubMed: 17322368]
49. Leor J, Rozen L, Zuloff-Shani A, Feinberg MS, Amsalem Y, Barbash IM, et al. Ex vivo activated human macrophages improve healing, remodeling, and function of the infarcted heart. Circulation. 2006; 114:I94–100. [PubMed: 16820652]
50. Nakajima T, Hishikari K, Ogawa M, Watanabe R, Suzuki J, Nagashima A, et al. Clarithromycin attenuates myocardial ischemia-reperfusion injury. Expert Opin Ther Targets. 2010; 14:881–93. [PubMed: 20662614]

51. Mosser DM, Edwards JP. Exploring the full spectrum of macrophage activation. Nat Rev Immunol. 2008; 8:958–69. [PubMed: 19029990]

52. Fazel S, Cimini M, Chen L, Li S, Angoulvant D, Fedak P, et al. Cardioprotective c-kit+ cells are from the bone marrow and regulate the myocardial balance of angiogenic cytokines. J Clin Invest. 2006; 116:1865–77. [PubMed: 16823487]

53. Rota M, Kajstura J, Hosoda T, Bearzi C, Vitale S, Esposito G, et al. Bone marrow cells adopt the cardiomyogenic fate in vivo. Proc Natl Acad Sci U S A. 2007; 104:17783–8. [PubMed: 17965233]

A

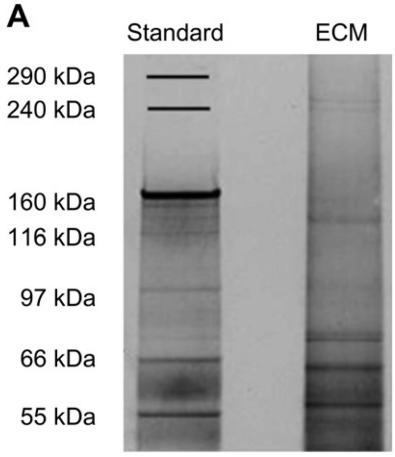

B

Component	Value (per mg of ECM)
FGF-2	72.7 ± 10.7 pg
PDGF-BB	80.9 ± 6.60 pg
IGF-1	1.23 ± 0.21 ng
VEGF	0.79 ± 0.26 pg
TGFβ1	446 ± 24.9 pg
sGAG	1.61 ± 0.07 ug

Fig. 1.

Composition of BM-ECM and MC gel. (A) SDS-PAGE of BM-ECM after purification. Silver staining was utilized to visualize the protein bands. Molecular weight standard markers indicate size. A total of 3 μg ECM was separated on a 3–8% Tris-acetate gel (Biorad Laboratories) in XT Tricine running buffer, and stained with silver stain. (B) Composition of BM-ECM, as determined by porcine ELISA and Blyscan kits.

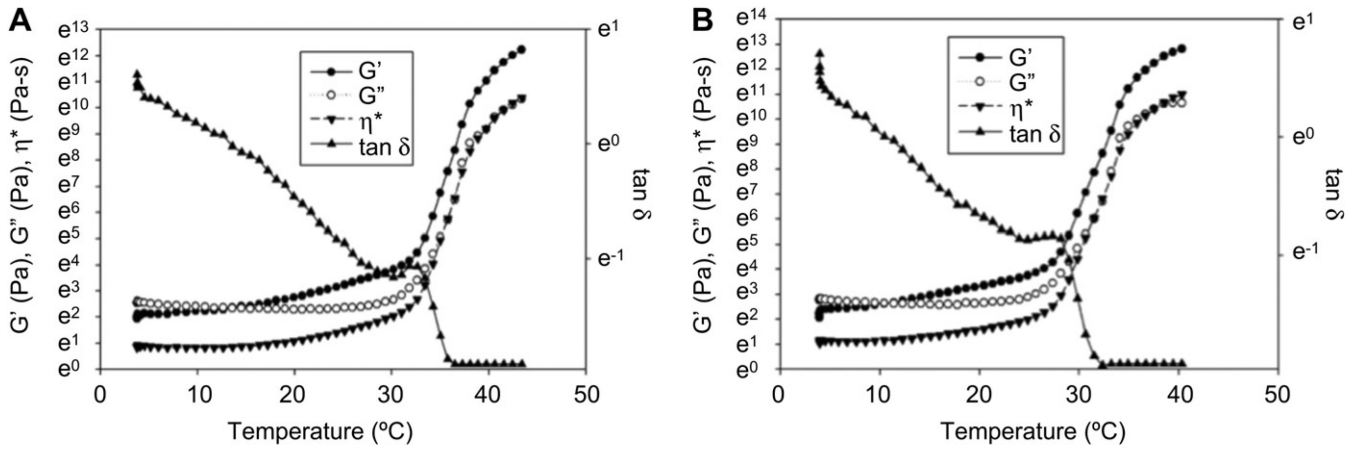

Fig. 2.

Rheological behavior of MC and ECM-MC. (A) 8wt% MC and (B) 8wt% MC containing 300 μg/mL BM-ECM. Storage modulus, loss modulus, and dynamic viscosity are plotted as a function of temperature (γ 2%, ω 1Hz). tan δ values are plotted on the right-hand side of the graphs.

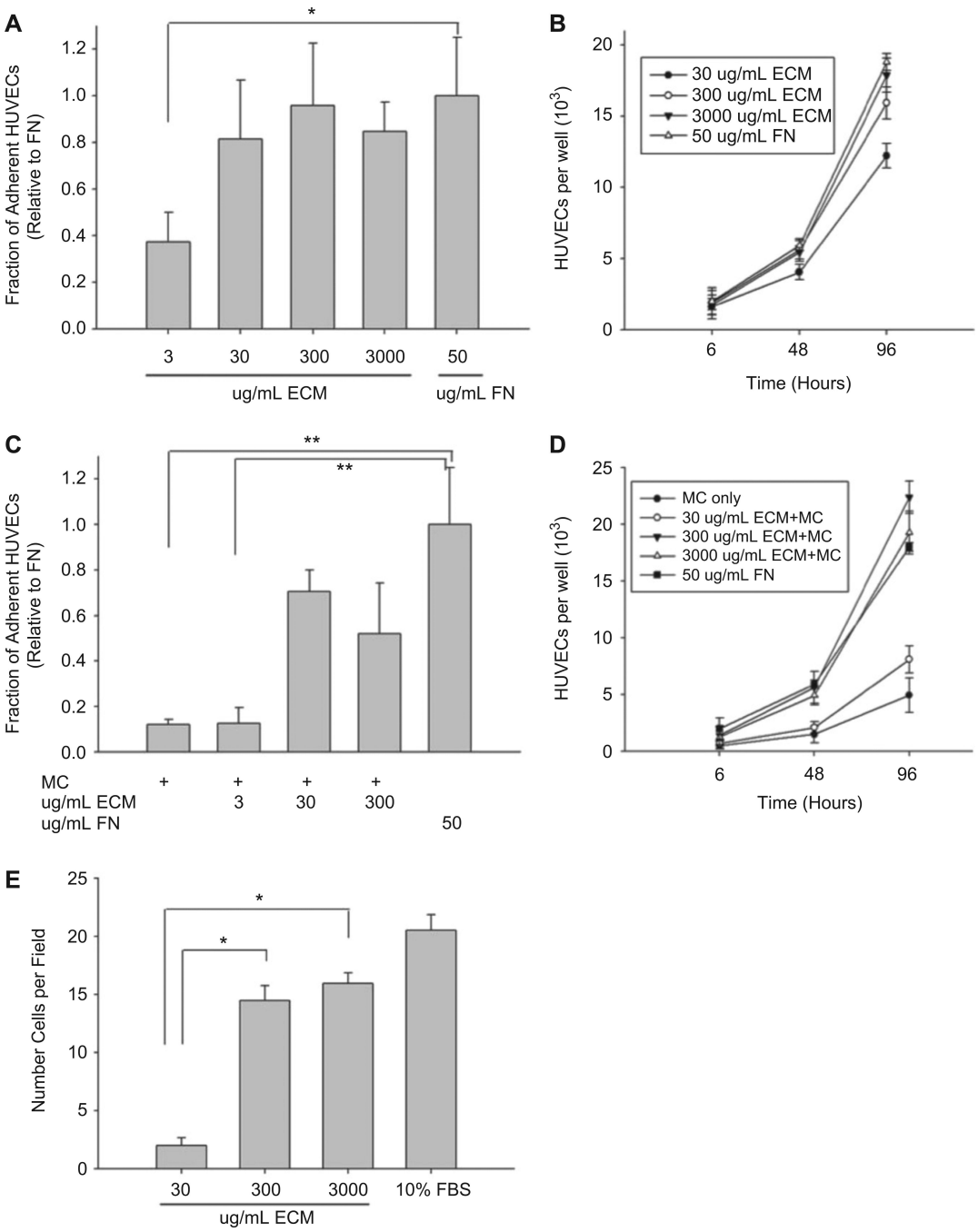

Fig. 3.

Cell adhesion and proliferation on BM-ECM. (A) 2-h HUVEC adhesion onto BM-ECM dilutions that were adsorbed overnight at 4 °C. Cells were seeded at a density of 50,000 cells per well in media containing no serum. Fibronectin adsorbed onto the non-tissue culture-treated 48-well plates served as the positive control. All data was normalized to the fibronectin (FN) control. (B) HUVEC proliferation over a 4-day period was followed. Cells were seeded at a density of 2000 cells per well for 6 h. Unbound cells were removed with media washes and substrate-bound cells were maintained in culture for 48 h and 96 h in serum-containing media. (C) 2-h HUVEC adhesion on 8wt% MC gels containing increasing ECM concentrations. (D) HUVEC proliferation on 8 wt% MC-ECM gels. (E) Haptotactic

migration assay, with 10% FBS serving as the positive control. The average number of migrated cells in six randomly chosen fields of view (40× magnification) per insert was quantified (*$p < 0.05$, **$p < 0.01$).

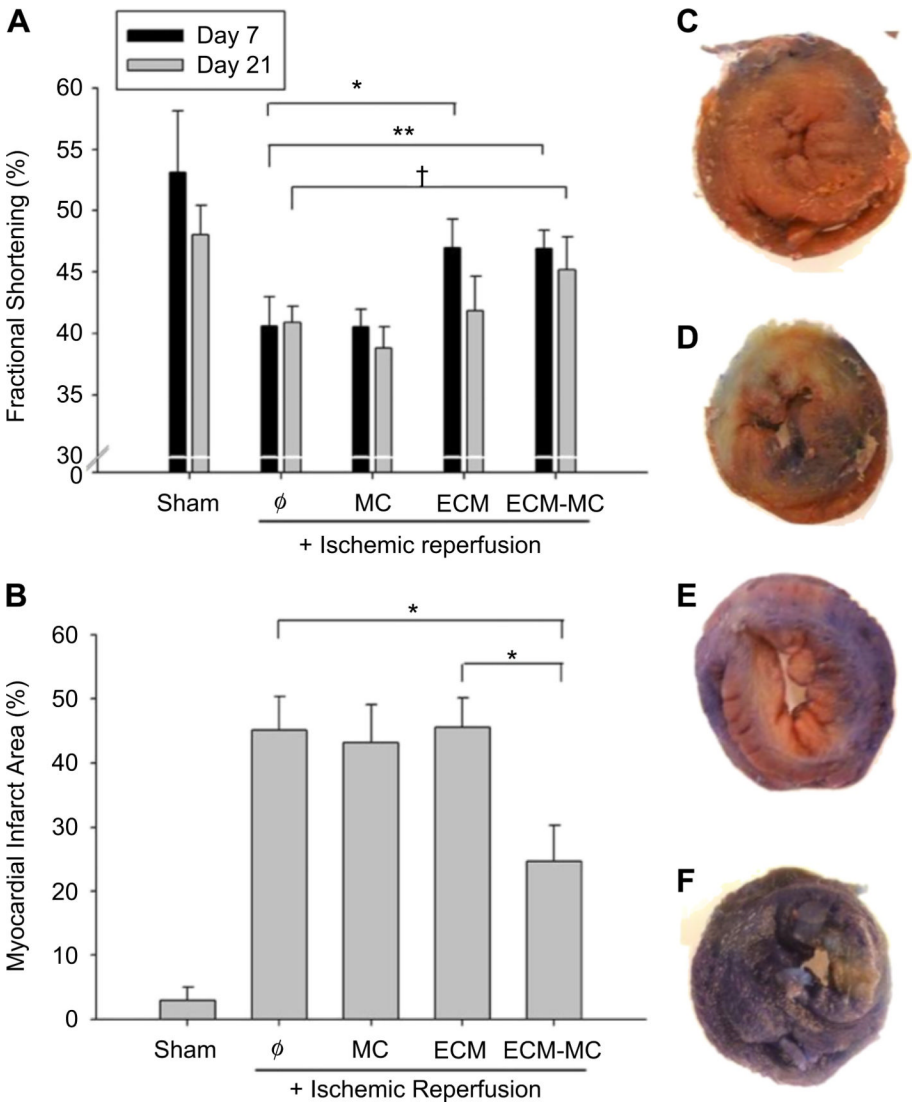

Fig. 4.

ECM-MC therapy results in improved cardiac function and reduced infarct area. Injected material consisted of 4 mg of MC and/or 15 μg of BM-ECM. (A) Cardiac function was assessed using echocardiography 7 and 21 d postinfarction, and dimensions of the heart were measured. Specifically, fractional shortening was derived from the end-diastolic dimension and end-systolic dimension (*$p < 0.05$, **$p < 0.01$, †$p = 0.05$). (B) Myocardial infarct area was assessed 24 h post-IR, and was defined as infarcted area divided by the ischemic area at risk. Representative images for (C) ischemic reperfusion only, (D) MC only, (E) BM-ECM only, and (F) ECM-MC delivery (*$p < 0.05$). For all studies, 4 rats were enrolled per treatment group.

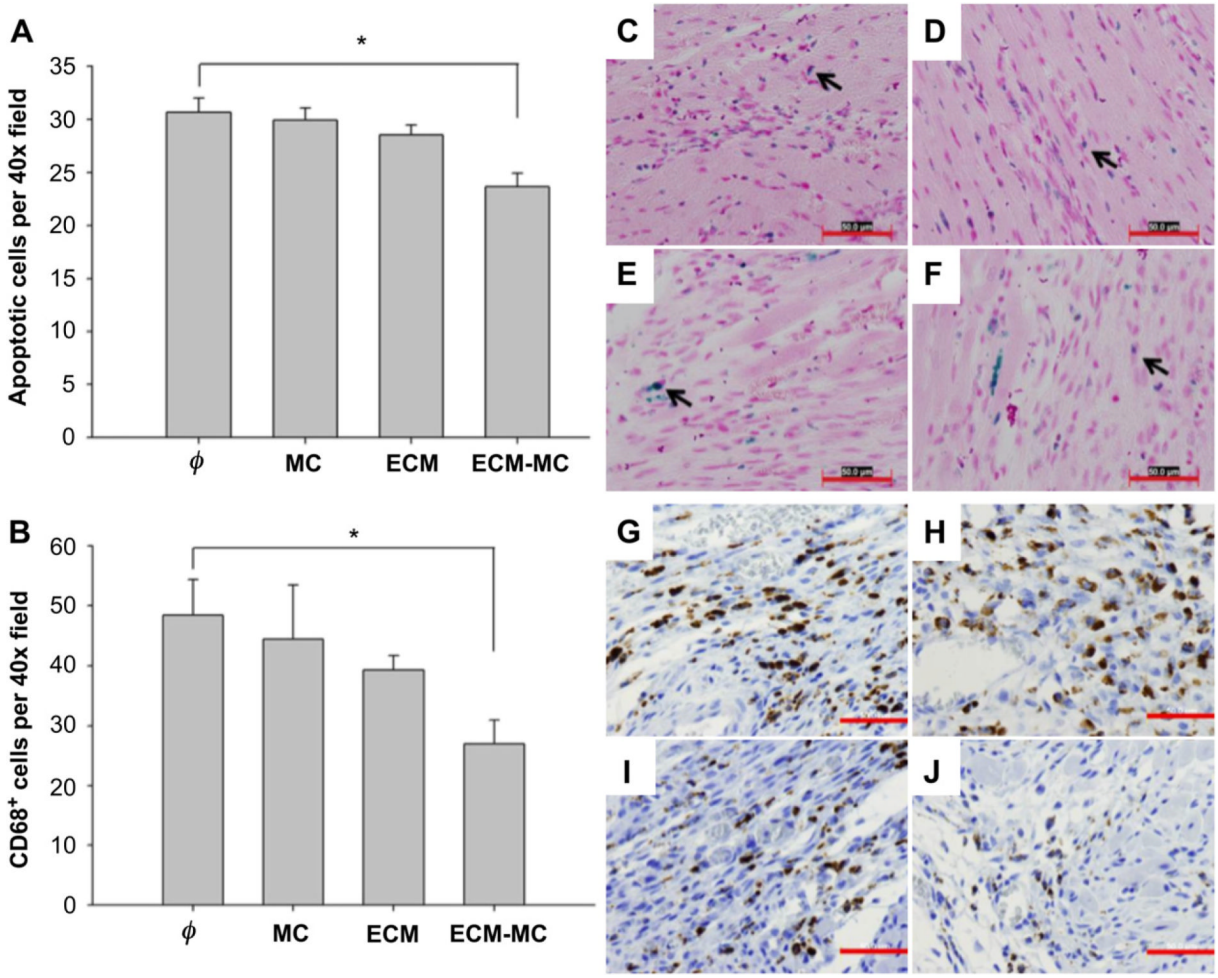

Fig. 5.

ECM-MC reduces the number of apoptotic cells (A) and decreases macrophage infiltration into the border zone (B). The left-ventricular free wall was analyzed 7 days after ischemic injury for apoptotic cells (C–F) and macrophages (G–J) at the border zone. Representative images of IR alone (C, G), IR + MC treatment (D, H), IR + BM-ECM treatment (E, I), and IR + ECM-MC treatment (F, J) were analyzed at the border zone in a blind manner (*$p <$ 0.05 compared to IR control). Four rats were enrolled per treatment group and three sections selected for each tissue sample. Apoptotic cells were CardioTACS *in situ* apoptosis detection kit (Trevigen) and macrophages with CD68 monoclonal antibody (Abcam). Four different fields (40×) in each section were recorded. Red bars signify 50 μm. (For interpretation of the references to color in this figure legend, the reader is referred to the web version of this article.)

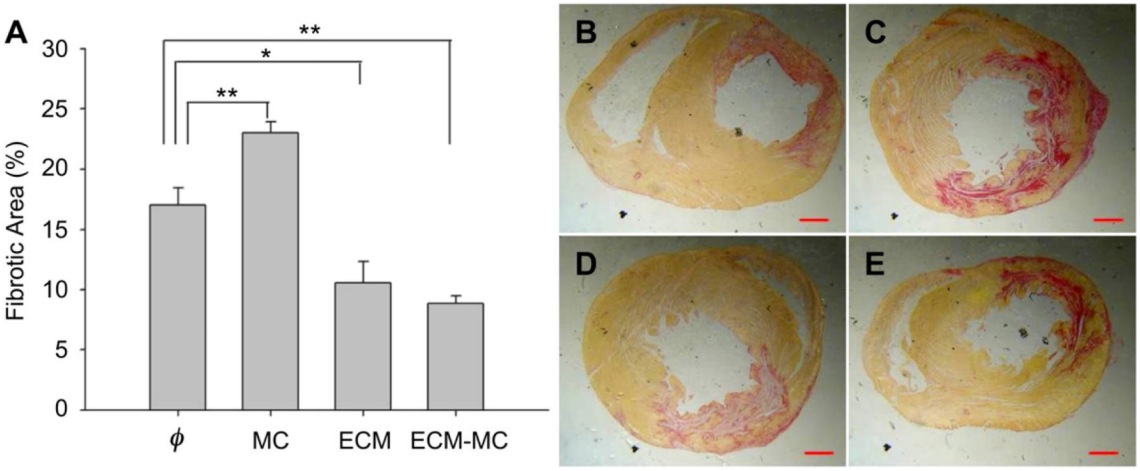

Fig. 6.

(A) ECM-MC therapy results in reduced fibrotic area. Injected material consisted of 4 mg of MC and/or 15 μg of BM-ECM. The left-ventricular free wall was analyzed 21 days after ischemic injury for fibrosis using collagen-specific Picrosirius Red stain. Representative images of IR alone (B), IR + MC treatment (C), IR + ECM treatment (D), and IR + ECM-MC treatment (E) were analyzed in a blind manner (*$p < 0.05$ and **$p < 0.01$ compared to IR control). Four rats were enrolled in each treatment group and three sections selected for each tissue sample. Red bars signify 1 mm. (For interpretation of the references to color in this figure legend, the reader is referred to the web version of this article.)

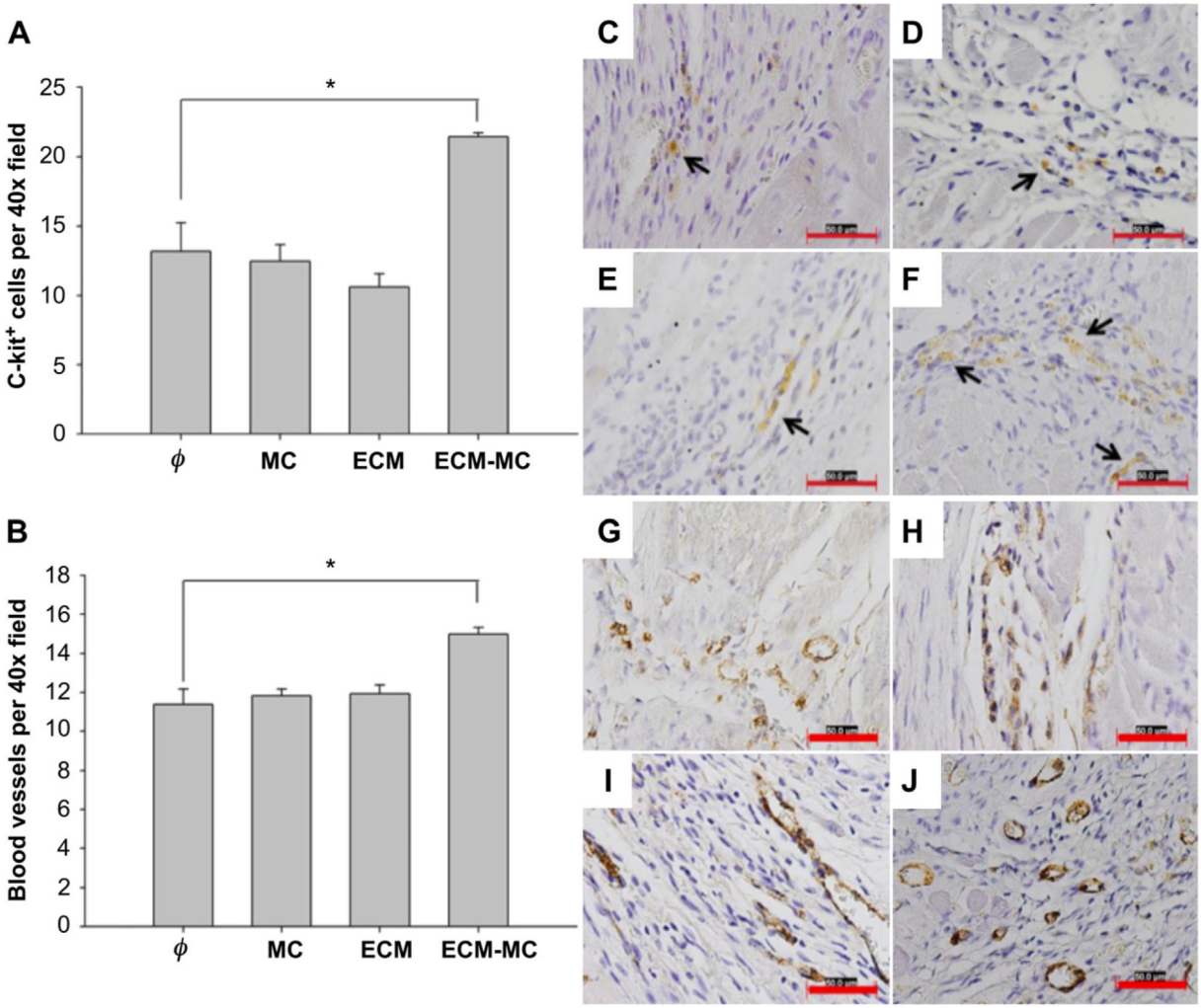

Fig. 7.

ECM-MC therapy promotes stem cell mobilization (A) and angiogenesis (B). Injected material consisted of 4 mg of MC and/or 15 μg of ECM. The left-ventricular free wall was analyzed 21 days after ischemic injury for c-kit-positive cells, identified with H-300 c-kit antibody (C–F), or for Von Willebrand Factor-stained cells (Abcam, ab6994) (G–J). Representative images of IR alone (C, G), IR + MC treatment (D, H), IR + BM-ECM treatment (E, I), and IR + ECM-MC treatment (F, J) were analyzed for cell counts or blood vessel density in a blind manner (*$p < 0.05$ compared to IR control). Four rats were enrolled per treatment group and three sections selected for each tissue sample. Four different fields (40×) in each section were assessed. Red bars signify 50 μm. Black arrows point to c-kit staining. (For interpretation of the references to color in this figure legend, the reader is referred to the web version of this article.)